Rapid Evolution of Resistance and Tolerance Leads to Variable Host Recoveries following Disease-Induced Declines

Mark Q. Wilber,1,* Joseph A. DeMarchi,1 Cheryl J. Briggs,2 and Sabrina Streipert3

1. School of Natural Resources, University of Tennessee Institute of Agriculture, Knoxville, Tennessee 37996; 2. Ecology, Evolution, and Marine Biology, University of California, Santa Barbara, California 93106; 3. Department of Mathematics, University of Pittsburgh, Pittsburgh, Pennsylvania 15260

Submitted July 21, 2023; Accepted January 5, 2024; Electronically published March 26, 2024 Online enhancements: supplemental PDF.

ABSTRACT: Recoveries of populations that have suffered severe disease-induced declines are being observed across disparate taxa. Yet we lack theoretical understanding of the drivers and dynamics of recovery in host populations and communities impacted by infectious disease. Motivated by disease-induced declines and nascent recoveries in amphibians, we developed a model to ask the following question: How does the rapid evolution of different host defense strategies affect the transient recovery trajectories of hosts following pathogen invasion and disease-induced declines? We found that while host life history is predictably a major driver of variability in population recovery trajectories (including declines and recoveries), populations that use different host defense strategies (i.e., tolerance, avoidance resistance, and intensity-reduction resistance) experience notably different recoveries. In single-species host populations, populations evolving tolerance recovered on average four times slower than populations evolving resistance. Moreover, while populations using avoidance resistance strategies had the fastest potential recovery rates, these populations could get trapped in long transient states at low abundance prior to recovery. In contrast, the recovery of populations evolving intensity-reduction resistance strategies were more consistent across ecological contexts. Overall, host defense strategies strongly affect the transient dynamics of population recovery and may affect the ultimate fate of real populations recovering from disease-induced declines.

Keywords: disease-induced declines, recovery, resilience, tolerance, amphibians, chytrid fungus.

* Corresponding author; email: mwilber@utk.edu.

ORCIDs: Wilber, https://orcid.org/0000-0002-8274-8025; Briggs, https://orcid.org/0000-0001-8674-5385; Streipert, https://orcid.org/0000-0002-5380-8818.

Introduction

Over the past two decades, severe declines in amphibians, bats, sea stars, Tasmanian devils, and other taxa have highlighted the sometimes devastating effects that pathogens can have on host populations (Blehert et al. 2008; Vredenburg et al. 2010; Langwig et al. 2016; Scheele et al. 2019; Cunningham et al. 2021; Hoyt et al. 2021). Stories of devastating declines have recently been interspersed with stories of recovery, where host populations and communities are rebounding following disease-induced declines (Voyles et al. 2018; Gignoux-Wolfsohn et al. 2021). The potential mechanisms leading to these recoveries include changes in host reproductive strategies (Brannelly et al. 2021), changes in host resistance or tolerance (Epstein et al. 2016), changes in pathogen virulence (Berngruber et al. 2013; Osnas et al. 2015), and density-driven changes in transmission rates (Tobler et al. 2012), but mechanisms of recovery in epizoological systems are only beginning to be explored. Questions of immediate relevance for ecology and conservation are as follows: When will populations and communities start recovering following diseaseinduced declines? What is the rate of population and community recovery? And will populations or communities recover to predecline states?

The recovery of host populations in disease ecology is often attributed to four processes: the evolution of the pathogen or the host (Kerr 2012), epidemic fade-out of the pathogen due to density-dependent reductions in transmission (Ballard et al. 2016; Searle and Christie 2021), the migration or assisted movement of resistant individuals to the focal population (Mendelson et al. 2019), and compensatory recruitment following disease-induced declines (Brannelly

et al. 2021). Host evolution in the form of evolutionary rescue has recently been proposed as a mechanism of recovery for populations following disease-induced declines (Golas et al. 2021; Searle and Christie 2021). It posits that evolutionary changes in the host population due to selection pressure from the pathogen contribute to a reversal of disease-induced declines and promote host recovery. While previous evolutionary approaches in disease ecology have often (but certainly not exclusively; Epstein et al. 2016; Byrne et al. 2021) focused on the evolution of the pathogen (Anderson and May 1982; Alizon et al. 2009; Lion and Metz 2018), evolutionary rescue of a host population assumes that rescue occurs as a result of heritable changes in the host while the pathogen is left relatively unchanged. Evidence for evolutionary rescue has been putatively observed in host taxa undergoing dramatic disease-induced declines, such as amphibians due to chytridiomycosis (Di-Renzo et al. 2018; Knapp et al. 2023), black-lipped abalone affected by herpes virus (Holland et al. 2022), bats declining from white-nose syndrome (Gignoux-Wolfsohn et al. 2021), and prairie dogs suffering from plague epidemics (Golas et al. 2021). Moreover, recent findings suggest that vertebrate taxa may have substantially more additive genetic variation in fitness-related traits than previously thought (Bonnet et al. 2022), supporting the potential role of host evolution in recovery dynamics.

There are two general defense strategies that host populations could evolve to combat disease and recover from disease-induced declines: resistance and tolerance (Raberg et al. 2009). Resistance defines the ability of a host to reduce, remove, or prevent infection and includes processes such as increased recovery rate from infection, reduction of pathogen intensity once infected, and avoidance of infection (Miller et al. 2007; Boots et al. 2009). In contrast, tolerance defines the ability to limit the negative fitness effects of infection without directly affecting infection itself (Raberg et al. 2009). Tolerance mechanisms could include controlling cellular damage induced by a host immune response to reduce host mortality rate (Medzhitov et al. 2012) or compensating for disease-induced mortality on host fitness by increasing reproductive rates (Gandon et al. 2002). The long-term outcomes of resistance and tolerance evolution have been extensively explored, and we summarize some key findings here (for a thorough review, see Boots et al. 2009).

Resistance and tolerance strategies result in different degrees of long-term genetic polymorphism in host defense traits. While tolerance strategies can become fixed within a population, resistance strategies tend to maintain variability (Antonovics and Thrall 1994; Boots and Bowers 1999; Roy and Kirchner 2000). Moreover, the degree of polymorphism in resistance traits following selection depends strongly on host life history, with longer-

lived hosts generally having less polymorphism than shorter-lived hosts (Bruns et al. 2015). In addition, tradeoffs between host defense and other aspects of host fitness, such as reproduction, have drastic affects on the evolutionary dynamics of host defense (Boots et al. 2009; Duffy and Forde 2009). For example, trade-offs between host resistance and fecundity (e.g., increases in host resistance decrease fecundity) tend to promote polymorphism in resistance traits (Boots and Haraguchi 1999; Roy and Kirchner 2000). This can lead to dynamic fluctuations in pathogen prevalence, as high-resistance and low-resistance phenotypes experience different fitness advantages in high-prevalence compared with low-prevalence environments (Roy and Kirchner 2000). Despite the substantial theoretical progress made on the long-term evolutionary dynamics of resistance and tolerance strategies, we know little about how the rapid transient evolution of host defense drives host recovery dynamics following the invasion of a pathogen (but for work on rapid evolutionary dynamics of resistance and tolerance, see Gandon and Day 2009). Thus, our motivating question for this study is the following: How does the rapid evolution of different host defense strategies affect the transient recovery trajectories of hosts following pathogen invasion and disease-induced declines?

Recovery is a component of a system's resilience (Neubert and Caswell 1997; Hodgson et al. 2015; Ingrisch and Bahn 2018). There are at least four characteristics of resilience that relate to the dynamics of population recovery in hostpathogen systems (Ingrisch and Bahn 2018; fig. 1): (i) the time it takes a population to reverse ongoing diseaseinduced declines, (ii) the magnitude of decline at this reversal, (iii) the time it takes a population to reach a new endemic attractor following this reversal, and (iv) the timeaveraged magnitude of this new attractor relative to the predecline attractor. Versions of these metrics have been described previously to understand the resilience of ecological systems and have been broadly defined as related to either resistance (i, ii; different from "resistance" defined in terms of host defenses sensu Raberg et al. 2009) or recovery (iii, iv) that together define a system's resilience (Neubert and Caswell 1997; Hodgson et al. 2015; Ingrisch and Bahn 2018; Capdevila et al. 2020). By recognizing the parallels between host recovery following disease-induced declines and resilience, we precisely define "host population recovery trajectories" as the four measurable characteristics described above (fig. 1) and quantitatively explore the impact of rapid evolution of resistance and tolerance on these dimensions of host population recovery.

While our focus is on the effects of host defense strategies on recovery trajectories following pathogen invasion, previous theory on demographic resilience has emphasized the importance of host life history on the transient dynamics of population recovery following perturbations (Capdevila

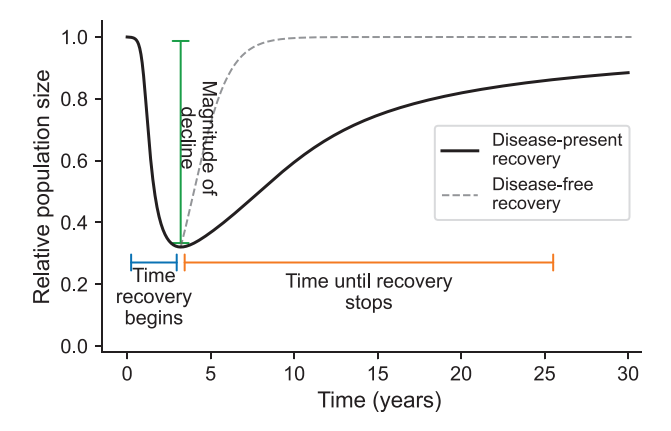


Figure 1: Example recovery trajectory (black line) of a host population with initial variability in tolerance. The dashed line indicates the recovery of a population that experienced an equivalent decline in the absence of disease. The blue line indicates when host recovery begins. The orange line indicates the time it takes a population to recover to its predecline population size (or some prespecified population size). The green vertical line gives the relative magnitude of the population decline before recovery begins. Together, these three attributes define the recovery trajectory. Our goal is to understand how host life history, pathogen life history, variability in host defenses, and defense-fecundity trade-offs affect population recovery trajectories in the presence of a pathogen.

et al. 2020; White et al. 2022). However, this theory was developed for nonevolving hosts and pulse disturbances, making it less applicable to our study, which involves evolving hosts and press disturbances. Nevertheless, we still expect host life history strategy (e.g., slow vs. fast hosts, where "slow" refers to hosts with long life spans and slow reproductive rates and "fast" refers to hosts with short life spans and fast reproduction; Valenzuela-Sánchez et al. 2021) to play a central role in the recovery trajectories of rapidly evolving host populations after disease-induced declines. Therefore, we aim to confirm this intuition and control for host life history when assessing the role of defense strategies on recovery trajectories. While incorporating disease and evolution into demographic resilience theory is beyond the scope of this study, our findings set the stage for its future integration.

Here, we use an epidemiological-evolutionary model motivated by an empirical host-pathogen system to test how different forms of host defense affect the recovery trajectories in rapidly evolving host populations following disease invasions and declines. We ask three questions. First, does host life history consistently affect recovery trajectories under different host defense strategies? Second, how do recovery trajectories differ between host populations evolving resistance or tolerance defense strategies? Third, do trade-offs between host defense and host fitness alter the effects of host defense strategies on recovery trajectories?

Empirical Motivation: Amphibian Declines and Recoveries following Disease-Induced Declines from a Fungal Pathogen

The biological motivation for our analyses are amphibian populations and communities that have experienced disease-induced declines due to the amphibian chytrid fungus Batrachochytrium dendrobatidis (Bd). Bd is a fungal pathogen that has caused the declines and extinctions of hundreds of amphibian species around the world (Scheele et al. 2019). However, some amphibian populations and species feared doomed to disease-induced extinction have persisted and begun to recover (Tobler et al. 2012; Knapp et al. 2016; Voyles et al. 2018). In at least two recovering systems in California and in El Cope, Panama, amphibian populations and communities have begun to recover in the presence of Bd, and there is little evidence that Bd has experienced a reduction in virulence, suggesting that some form of evolved host defense may be driving recovery (Knapp et al. 2016, 2023; Joseph and Knapp 2018; Voyles et al. 2018; Byrne et al. 2021).

Motivated by amphibian-Bd systems, we make five key assumptions in our models. First, we focus our analyses on host evolution while assuming that the pathogen remains unchanged throughout the recovery trajectory, consistent with empirical findings in California and Panama. Second, we model pathogen transmission through an environmental pathogen pool, which accounts for the transmission biology of amphibian-Bd systems where Bd zoospores are shed from the skin of infected amphibian hosts, travel through the water, and infect other amphibian hosts (Kilpatrick et al. 2010). This also allows us to implicitly consider the effects of pathogen infection intensity on host recovery dynamics (Vredenburg et al. 2010; Knapp et al. 2016)—an important characteristic in amphibian-Bd dynamics—by modeling pathogen shedding rate. Third, we consider resistance and tolerance traits to be massively polygenic, reflecting our understanding of resistance and tolerance in amphibian-Bd systems (namely, that we have not found a single gene highly predictive of resistance or tolerance; Byrne et al. 2021; Knapp et al. 2023). Thus, we use continuous trait space and do not consider bimorphic traits, dominance, or gene-for-gene models (Roy and Kirchner 2000; Agrawal and Lively 2002). Fourth, as Bd is highly virulent, we assume that host mutation does not play a significant role in rescue dynamics (from theory, given a larger reduction in host fitness in a new environment, the more likely standing variation is to rescue a population; Orr and Unckless 2014). Instead, we consider existing standing variation in host defense as the basis for selection (Bonnet et al. 2022). However, our approach can easily be extended to account for host mutation. Finally, Bd infects multiple amphibian species. We initially develop a model

with a single host species but return to amphibian communities in the discussion section.

Given these assumptions, we develop a simple model to (i) gain semianalytical understanding of the drivers of host recovery trajectories and (ii) extensively explore parameter space to compare recovery trajectories under different host defense strategies. Although our model ignores certain aspects of amphibian-Bd interactions (such as stage structure, complex life history, and explicit intensitydependent infection dynamics), it provides a foundation for generating predictions about the ecological, epidemiological, and evolutionary factors driving amphibian recovery trajectories. Moreover, its generality provides insights into evolution and recovery dynamics in other host-pathogen systems with environmental transmission, such as bats and white-nose syndrome (e.g., Gignoux-Wolfsohn et al. 2021). When pathogen decay rate in the environment is fast relative to transmission, our model captures standard density-dependent transmission such that our results are also applicable to host-parasite systems with direct transmission (Cortez and Duffy 2021).

Model Description

We consider a host population capable of evolving increased resistance or tolerance in response to pathogen invasion. Our aim is to examine how three aspects of the population recovery trajectory—time until recovery begins, magnitude of decline, and time until recovery stops (fig. 1)—differ between host populations that rapidly evolve resistance and tolerance following disease invasion. In contrast to previous research on the long-term evolutionary dynamics of resistance and tolerance (Miller et al. 2005, 2006; Boots et al. 2009), we focus on a single selective sweep and the transient dynamics of population recovery following pathogen invasion and disease-induced declines

We assume a population of susceptible (S) and infected (I) hosts with transmission occurring through an environmental pathogen pool (Z). Consistent with previous literature (Roy and Kirchner 2000; Miller et al. 2006, 2007; Boots et al. 2009), we define host tolerance in terms of disease-induced mortality α , where $1/\alpha$ defines tolerance. Note that in our model below, we explicitly account for pathogen shedding from infected hosts. Given an assumption that α is positively correlated with within-host infection intensity, which in turn is positively correlated with pathogen shedding rate ω , it follows that varying α among hosts while holding pathogen shedding rate constant is equivalent to a tolerance mechanism (i.e., a host changes its ability to survive with the pathogen without affecting pathogen intensity and shedding rate).

We consider two distinct mechanisms of host resistance: avoidance resistance and intensity-reduction resistance (Miller et al. 2005; Boots et al. 2009). Consistent with previous literature (Boots and Bowers 1999; Roy and Kirchner 2000), we define avoidance resistance in terms of the transmission rate β , where $1/\beta$ quantifies avoidance resistance. We define intensity-reduction resistance by allowing for variability in disease-induced mortality among hosts but also allowing pathogen shedding rate to be an increasing function of $\hat{\alpha}$, $\omega(\hat{\alpha}) = \phi \hat{\alpha}$ (Miller et al. 2005). For clarity throughout, we refer to disease-induced mortality as $\hat{\alpha}$ rather than α when we are referencing the intensity-reduction resistance model, where shedding rate varies with diseaseinduced mortality. For intensity-reduction resistance, we assume that reducing $\hat{\alpha}$ is a direct result of reducing withinhost infection intensity, which also leads to a reduction in pathogen shedding rate. In amphibian-Bd systems we have evidence that tolerance, avoidance resistance, and intensityreduction resistance are all potential defense strategies (McMahon et al. 2014; Knapp et al. 2016, 2022). However, at this early stage of observing amphibian recoveries following disease-induced declines, we only have strong evidence that tolerance and intensity-reduction resistance are heritable strategies that can evolve and can drive host recoveries (Knapp et al. 2023).

To account for variability in tolerance and resistance among hosts, we allow α , β , and $\hat{\alpha}$ to vary continuously among hosts. Thus, in the tolerance model $N(\alpha,t)d\alpha$ and $I(\alpha,t)d\alpha$ refer to the total density of hosts (N=S+I) and total density of infected hosts with α between α and $\alpha+d\alpha$. In the avoidance resistance models, $N(\beta,t)d\beta$ and $I(\beta,t)d\beta$ refer to the total density of hosts and total density of infected hosts with β between β and $\beta+d\beta$ (defined equivalently for intensity-reduction resistance, $\hat{\alpha}$).

We also assume that lower α , lower β , or lower $\hat{\alpha}$ (higher tolerance, avoidance resistance, and intensity-reduction resistance, respectively) can come at a cost to host fitness such that host birth rate r is a function of α for tolerance $(r(\alpha))$ and β or $\hat{\alpha}$ for resistance $(r(\beta))$ or $r(\hat{\alpha})$. While we do not have data to assess whether such a trade-off exists in amphibian-Bd systems, this trade-off is a standard assumption in evolutionary models of tolerance and resistance (Roy and Kirchner 2000; Duffy and Forde 2009) and has been empirically identified in other systems (Miller et al. 2007). One of our goals is to understand whether fitness-defense trade-offs affect host recovery trajectories under different defense strategies. Therefore, we include this trade-off in our models, recognizing that obtaining empirical data on this trade-off is a key unknown in amphibian-Bd systems (Wilber et al. 2019). Finally, for simplicity we assume perfect inheritance (e.g., parents with tolerance $1/\alpha$ produce offspring with tolerance $1/\alpha$). As we are ultimately interested in describing the general anatomy of recovery trajectories, these simple genetic assumptions provide a reasonable starting point.

Our model is

$$\frac{dN(x,t)}{dt} = [r(x) - \delta N(t)]N(x,t)
- \mu N(x,t) - \alpha I(x,t),
\frac{dI(x,t)}{dt} = \beta ZS(x,t) - I(x,t)(\mu + \alpha + \gamma),
\frac{dZ}{dt} = \int_{x} \omega(x')I(x',t)dx' - \mu_{z}Z.$$
(1)

The parameter μ is intrinsic host death rate, and δ is the strength of the density-dependent reduction in host birth rate due to intraspecific competition. The epidemiological parameters include the disease-induced mortality rate α , the transmission parameter β , the recovery rate γ , the rate at which individuals release pathogen into the environment $\omega(x)$, and the pathogen mortality rate μ_Z , where all parameters are positive. We replace x with α , β , or $\hat{\alpha}$ in N(x,t), I(x,t), r(x), $\omega(x)$, and the integral to obtain the tolerance, avoidance resistance, or intensity-reduction resistance model, respectively (supplemental PDF, sec. S1). When x is α or β , $\omega(x) = \omega$. When x is $\hat{\alpha}$, $\omega(\hat{\alpha}) = \phi \hat{\alpha}$ (i.e., shedding rate is proportional to disease-induced mortality rate).

Finally, an assumption that we make in the model is that the depletion of pathogen from the environment upon transmission is minimal. In the accompanying code available on Zenodo (https://zenodo.org/doi/10.5281/zenodo .10475490; see the script anatomy_of_recovery_analysis .ipynb, 1.2.3), we show that including pathogen depletion (by adding the term $-\beta ZN$ to dZ/dt in eq. [1] with intensityreduction resistance) negligibly influences host recovery trajectories within the parameter space we explore. Thus, we chose to ignore pathogen depletion in our subsequent analyses.

Model Reduction: Moment Closure Approximations

To gain semianalytical insight into equation (1) for different tolerance and resistance strategies, we used a moment closure approximation to derive explicit equations for the dynamics of the mean and variance of α , β , and $\hat{\alpha}$ with respect to I and N (Bolker and Pacala 1997; a full description of the derivations is given in sec. S1 of the supplemental PDF). The moment closure approach is a generalization of the population genetics models previously used in evolutionary epidemiology to explore the rapid evolutionary dynamics of hosts and pathogens (Day and Gandon 2007; Gandon and Day 2009). In contrast to population genetics models, which focus on the dynamics of mean traits assuming fixed variance (Day and Gandon 2007), modeling the dynamics of the trait variance requires some distributional assumptions. We assumed that the random variable $\alpha(t)$ ($\beta(t)$, $\hat{\alpha}(t)$) follows a gamma distribution at all times t with mean $\bar{\alpha}(t)$ ($\bar{\beta}(t)$, $\hat{\alpha}(t)$) and variance $Var(\alpha)(t)$ ($Var(\beta)(t)$, $Var(\hat{\alpha})(t)$). We chose a gamma distribution because it is a flexible distribution that is strictly positive and has convenient mathematical properties that allowed for closed-form expressions of our moment closure approximation (supplemental PDF, sec. S1). These moment closure approximations allowed us to relate our results directly to previous evolutionary epidemiological models and facilitated more expansive exploration of the parameter space than a direct analysis of equation (1). However, we confirmed that our moment closure approximations and discretized implementations of equation (1) (i.e., a model that did not assume a gamma-distributed trait) yielded equivalent results (see accompanying script anatomy_of_recovery_analysis.ipynbon on Zenodo).

To derive the moment closure equations for tolerance, we multiplied $N(\alpha, t)$ and $I(\alpha, t)$ in equation (1) by α^0, α^1 , and α^2 and integrated over α to derive the zeroth-moment (related to total host abundance), first-moment (equivalent to the mean in α), and second-moment (related to the variance in α) equations for N and I, respectively. We used an equivalent approach to derive moment closure equations for avoidance resistance β and intensityreduction resistance $\hat{\alpha}$ (supplemental PDF, sec. S1).

The moment closure equations we use to approximate our tolerance model are (supplemental PDF, sec. S1; assuming $r(\alpha) = r$; model with trade-off $r(\alpha)$ is given in sec. S2 of the supplemental PDF) as follows:

$$\begin{split} \frac{dN}{dt} &= rN - \delta N^2 - \mu N - \bar{\alpha}_N I, \\ \frac{dI}{dt} &= \beta Z S - (\mu + \gamma) I - \bar{\alpha}_N I, \\ \frac{dZ}{dt} &= \omega I - \mu_Z Z, \\ \frac{d\bar{\alpha}_N}{dt} &= -\frac{I}{N} \text{Var}(\alpha) = -\text{Cov}\left(\alpha, \alpha \frac{I(\alpha)}{N(\alpha)}\right), \\ \frac{d\text{Var}(\alpha)}{dt} &= -2 \frac{I}{N} \frac{\text{Var}(\alpha)^2}{\bar{\alpha}_N}, \end{split}$$

where $\bar{\alpha}_N$ is the mean value of α in the full population at time t and $Var(\alpha)$ is the variance in α at time t. The dynamics of mean tolerance in the full population $\bar{\alpha}_N$ can be expressed in terms of Price's equation describing the dynamics of a mean trait in a heterogeneous population (supplemental PDF, sec. S1; consistent with Day and Gandon 2007).

The moment closure equations we use to approximate our avoidance resistance model are (supplemental PDF, sec. S1; assuming $r(\beta) = r$; model with trade-off $r(\beta)$ is given in sec. S2 of the supplemental PDF) as follows:

$$\frac{dN}{dt} = rN - \delta N^2 - \mu N - I\alpha,$$

$$\frac{dI}{dt} = \bar{\beta}_N Z N - \bar{\beta}_I Z I - I(\mu + \alpha + \gamma),$$

$$\frac{dZ}{dt} = \omega I - \mu_z Z,$$

$$\frac{d\bar{\beta}_N}{dt} = -\frac{I}{N} \alpha (\bar{\beta}_I - \bar{\beta}_N) = -\alpha \text{Cov} \left(\beta, \frac{I(\beta)}{N(\beta)}\right),$$

$$\frac{d\bar{\beta}_I}{dt} = Z \frac{N}{I} \left(\nu_N - \bar{\beta}_I \bar{\beta}_N\right) - Z \left(\nu_I - \bar{\beta}_I^2\right),$$

$$\frac{d\nu_N}{dt} = -\frac{I}{N} \alpha (\nu_I - \nu_N),$$

$$\frac{d\nu_I}{dt} = Z \frac{N}{I} \left(E_N[\beta^3] - \nu_I \bar{\beta}_N\right) - Z \left(E_I[\beta^3] - \nu_I \bar{\beta}_I\right),$$

where $\bar{\beta}_N$ and $\bar{\beta}_I$ are the mean values of β in the full population and only in infected individuals, respectively. The state variables ν_N and ν_I are the second moments of β , and $\nu_N - \bar{\beta}_N^2$ and $\nu_I - \bar{\beta}_I^2$ are the variances of β in the full host population and infected individuals, respectively. The term $E_I[\beta^3]$ gives the third moment of the distribution of β in the infected population, and $E_N[\beta^3]$ gives the third moment of the distribution of β in the total population (using a gamma distribution, we can write the third moment in terms of the first and second moments; see sec. S1 of the supplemental PDF). Here, we can also express the change in the mean trait $\bar{\beta}_N$ using Price's equation (Day and Gandon 2007). While conceptually useful, this covariance formulation is less explicit about the fact that the dynamics of $\bar{\beta}_N$ depend on dynamic variance in β and $\bar{\beta}_I$.

Finally, the moment closure equations we use to approximate our intensity-reduction resistance model are (supplemental PDF, sec. S1; assuming $r(\hat{\alpha}) = r$; model with tradeoff $r(\hat{\alpha})$ is given in sec. S2 of the supplemental PDF) as follows:

$$\frac{dN}{dt} = rN - \delta N^2 - \mu N - I\bar{\alpha}_I,$$

$$\frac{dI}{dt} = \beta ZS - (\mu + \gamma)I - I\bar{\alpha}_I,$$

$$\frac{dZ}{dt} = \phi\bar{\alpha}_I I - \mu_z Z,$$

$$\frac{d\bar{\alpha}_N}{dt} = -\frac{I}{N} \left(v_I - \bar{\alpha}_N \bar{\alpha}_I \right) = -\text{Cov} \left(\hat{\alpha}, \hat{\alpha} \frac{I(\hat{\alpha})}{N(\hat{\alpha})} \right), \quad (4)$$

$$\frac{d\bar{\alpha}_I}{dt} = \beta Z \frac{N}{I} \left(\bar{\alpha}_N - \bar{\alpha}_I \right) - \left(v_I - \bar{\alpha}_I^2 \right),$$

$$\frac{dv_N}{dt} = -\frac{I}{N} \left(E_I[\hat{\alpha}^3] - v_N \bar{\alpha}_I \right),$$

$$\frac{dv_I}{dt} = \beta Z \frac{N}{I} (v_N - v_I) - \left(E_I[\hat{\alpha}^3] - v_I \bar{\alpha}_I \right).$$

The parameter ϕ is equal to $\omega/\hat{\alpha}_0$, where $\hat{\alpha}_0$ is the initial value of $\hat{\alpha}$ prior to host evolution. We set $\phi = \omega/\hat{\alpha}_0$ to ensure comparability among our different defense strategies. The other parameters are defined analogously to tolerance and avoidance resistance models. Similar to tolerance and avoidance resistance, we can also express the dynamics of mean $\hat{\alpha}_N$ in the form of Price's equation, relating the fitness gradient to the covariance between $\bar{\alpha}_N$ and the effect of infection on host fitness.

Model Analyses

To answer our three questions regarding host recoveries, we focused on three characteristics of the recovery trajectory (fig. 1): (i) the time from initial pathogen invasion to when recovery begins, (ii) the magnitude of decline in the host population following pathogen introduction (normalized on the basis of starting population size), and (iii) the time until a population is within 2% of its initial population size (where 2% is an arbitrary choice but does not affect our qualitative conclusions; fig. 1). These characteristics jointly describe the recovery trajectories and are the response variables in our subsequent analyses.

We performed a global sensitivity analysis (Marino et al. 2009) where we used Latin hypercube sampling to draw 10,000 stratified random samples for the following parameters in equations (2), (3), and (4): β , ω , μ_{z} , r, μ , δ , and α . When we were modeling tolerance or intensity-reduction resistance (eq. [2] or [4]), α represented the initial mean $\bar{\alpha}_N$ or $\bar{\alpha}_N$, respectively, at time t=0 immediately prior to pathogen invasion. Similarly, when we were modeling avoidance resistance (eq. [3]), β represented the initial mean $\bar{\beta}_N$ at time t=0 immediately prior to pathogen invasion. We also varied the initial coefficient of variation for α , $\hat{\alpha}$, or β to allow for different (but comparable) magnitudes of variability in tolerance or resistance prior to pathogen invasion. The range of each of the parameters that we explored is given in table 1.

After drawing parameters, we excluded all parameter combinations where the hosts could not persist (intrinsic host growth rate was less than zero) and the pathogen could not invade upon initial introduction (intrinsic pathogen growth rate was less than zero). As we were interested in host recovery trajectories following disease-induced declines, successful pathogen invasion was an essential criterion for our study. Moreover, given density-dependent transmission and a single-species host-pathogen system (our assumption in this study), deterministic, disease-induced extinction was impossible (supplemental PDF, sec. S4). However, disease-induced declines can reduce host density substantially, significantly augmenting stochastic extinction risk in natural populations (Wilber et al. 2019). Thus, only considering situations where host and pathogen growth

Table 1: Parameters and ranges used in global sensitivity

Parameter (units)	Range
Transmission rate β (area per year)	.053
Disease-induced mortality α (per year)	1-3
Pathogen shedding rate ω (pathogens per year)	100-1,000
Pathogen death rate μ_z (per year)	10-100
Metric of initial variability in host defense k	
(unitless)	.5-5
Per capita birth rate r (per year)	.1-10
Host death rate μ (per year)	.1-3
Intraspecific competition δ (area per year)	.15
Shedding rate to initial mortality rate ratio ϕ	
(unitless)	$\omega/lpha_0$

Note: For all models, we set loss of infection rate $\gamma = 0$.

rates were greater than zero captured all of the potential host recovery trajectories of interest.

For equation (1), the intrinsic host growth rate is given by $\lambda_{\text{host}} = r - \mu$, and the intrinsic pathogen growth rate is given by $\lambda_{\text{para}} = -((\bar{\alpha}_N^0 + \mu + \mu_z)/2) + ((4N^*\bar{\beta}_N^0\omega + (\bar{\alpha}_N^0 + \mu)^2 - 2(\bar{\alpha}_N^0 + \mu)\mu_z + \mu_z^2)^{1/2}/2)$, where $\bar{\alpha}_N^0$ and $\bar{\beta}_N^0$ represent the initial mean disease-induced mortality α and transmission β in the full population immediately prior to pathogen invasion. The term N^* is the host population at the disease-free equilibrium. We excluded all parameter combinations where pathogen $R_0 > 20$; R_0 is a unitless number of pathogen reproduction that is comparable among populations $(R_0 = (\bar{\beta}_N^0 N^* \omega)/(\bar{\alpha}_N^0 + \mu)\mu_z))$, and $R_0 > 20$ represents a borderline unrealistically large value for R_0 . That being said, we do examine the consequences of large R_0 on recovery trajectories below. On average, we performed our subsequent analyses on approximately 60% of the 10,000 parameter combinations that had median $R_0 = 5.4$ and R_0 25th and 75th percentiles of 2.81 and 9.89, respectively. For each parameter set, we simulated equations (2)– (4), generated a recovery trajectory, and calculated our three metrics of interest (fig. 1).

To answer our first question regarding whether host life history consistently affected host recovery trajectories, we calculated the partial correlation coefficients (PCCs) between $log(\lambda_{host})$ and each of our three log-transformed output metrics that jointly described our recovery trajectory (fig. 1). We also calculated PCCs for $\log(\lambda_{para})$ and log(initial coefficient of variation in α , β , or $\hat{\alpha}$) to further explain variation in simulated recovery trajectories. PCCs measure the correlation between a variable of interest and an outcome after accounting for the effects of all other variables (Marino et al. 2009). A higher absolute value of a PCC indicates that a particular input variable is more tightly correlated with the output, independent of all other inputs. We also ran a regression model where $\log(\lambda_{host})$, $\log(\lambda_{para})$, and $\log(\text{initial coefficient of variation in } \alpha \text{ or } \beta)$

were additive predictor variables and each log-transformed output variable related to the recovery trajectory was a response variable. We calculated the R^2 value of the resulting model to examine how much variance in attributes of the recovery trajectory was explained by host life history, pathogen growth rate, and initial variability in host defense.

To answer our second question regarding differences between recovery trajectories of populations using tolerance, avoidance resistance, or intensity-reduction resistance strategies, we performed paired comparisons between populations with identical starting parameters and variability in α , β , or $\hat{\alpha}$. We standardized variability between tolerant and resistant populations by ensuring that populations had the same starting variance in α , β , or $\hat{\alpha}$ relative to the mean starting value (i.e., populations had identical coefficient of variations in α , β , or $\hat{\alpha}$ immediately prior to pathogen invasion). We then compared how the time when recovery begins, the magnitude of decline, and the time until a population recovers to 2% of its initial population size differed between populations evolving tolerance, avoidance resistance, or intensity-reduction resistance.

To answer our third question regarding the effects of tradeoffs on recovery trajectories, we repeated the simulation analysis and compared populations with and without a trade-off in fecundity and host defense while keeping other parameters constant. We assessed the change in (i) time from pathogen invasion to recovery onset, (ii) magnitude of decline in host population after pathogen introduction, and (iii) time until the population reaches 2% of the equilibrium host abundance in the presence of a trade-off. We included a concave-down trade-off between host defense and fecundity as described in section S2 of the supplemental PDF. For the last item (iii), including a trade-off between host defense and fecundity yielded equilibrium host abundances following pathogen invasion that were less than host abundance prior to pathogen invasion. For models that were identical other than the presence of a trade-off, we measured the time until the population from either model was within 2% of the equilibrium host abundance in the presence of the trade-off. We examined populations with an initial coefficient of variation in α , β , or $\hat{\alpha}$ less than 0.1 (i.e., small variance relative to the mean), such that a population was experiencing no selection gradient on these traits prior to pathogen arrival.

Results

Question 1: Faster Life History Hosts Experience Smaller Disease-Induced Declines and Faster Recoveries Regardless of Host Defense Strategy

Host population recovery trajectories following pathogen invasion were predictably influenced by host life history

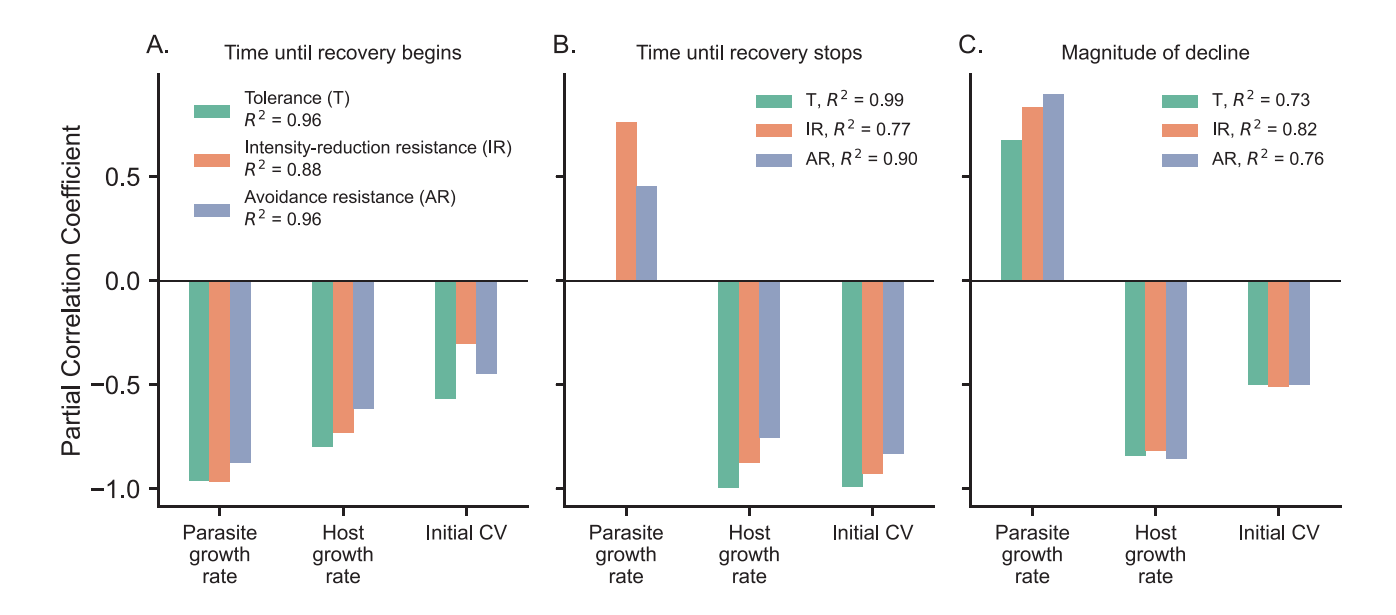


Figure 2: Effects of pathogen growth rate, host growth rate, and initial variability in α (tolerance), $\hat{\alpha}$ (intensity-reduction resistance), and β (avoidance resistance) on attributes of a host population's recovery trajectory. The bars in each plot show the partial correlation coefficients between (log) pathogen growth rate, (log) host growth rate, and (log) initial variability in α , $\hat{\alpha}$, and β and each attribute of the recovery trajectory. For a given host defense strategy and attribute of the recovery trajectory, the R^2 value gives the total amount of variation in the attribute of the recovery trajectory described by the multiple regression with all three variables (additive effects only). For example, for tolerance in A, $R^2 = 0.96$ means that a multiple regression with pathogen growth rate, host growth rate, and initial variability in α explains 96% of the variation in time until recovery begins. A, Sensitivity results for time until recovery begins. B, Sensitivity results for time until recovery stops. C, Sensitivity results for magnitude of decline. CV = coefficient of variation.

 (λ_{host}) . Across all three host defense strategies, populations of faster life history hosts experienced smaller disease-induced declines and faster recoveries (fig. 2). Notably, despite intrinsic host growth rate being highly predictive of recovery time, host populations evolving tolerance and resistance showed slower recovery compared with predictions from a disease-free scenario following an equivalent perturbation in an otherwise identical population (figs. 1, S1; figs. S1–S3 are available online).

Increasing initial standing variation in host defense traits impacted all three characteristics of the recovery trajectory, particularly reducing the time until recovery stops for all defense strategies (fig. 2). Finally, pathogen growth rate (λ_{para}) notably contributed to the magnitude of decline and time until recovery begins across defense strategies, explaining 17% and 84% of the variation, respectively (fig. 2). Interestingly, this implies that by quantifying initial parasite growth rate upon invasion, we may be able to predict characteristics of the host recovery trajectory, including the duration of disease-induced declines (fig. 2). In section S3 of the supplemental PDF, we use our tolerance model to derive additional analytical insight into the effects of initial standing variation, host life history, and pathogen growth rate on population recovery trajectories.

Question 2: Hosts Using Resistance Strategies Tend to Recover More Quickly Than Hosts Using Tolerance Strategies

For all host defense strategies, the dynamics of total population size are $dN/dt = N\rho(t)$, where $\rho(t)$ is the intrinsic host growth rate (i.e., fitness), $\rho(t) < 0$ indicates a declining population, and $\rho(t) > 0$ indicates a recovering population.

For hosts using a tolerance strategy,

$$\rho(t) = \rho(N, I, \bar{\alpha}) = \bar{r}_{\alpha}(t) - \delta N(t) - \mu - \bar{\alpha}_{I}(t) \frac{I(t)}{N(t)},$$
(5)

where \bar{r}_{α} is the average host growth rate, averaged over the instantaneous distribution of tolerance in the population; $\bar{\alpha}_{l}$ is the average tolerance level in only infected hosts; and I/N is pathogen prevalence in the host population.

For hosts using an intensity-reduction resistance strategy,

$$\rho(t) = \rho(N, I, \hat{\alpha}) = \bar{r}_{\hat{\alpha}}(t) - \delta N(t) - \mu - \hat{\alpha}_I(t) \frac{I(t)}{N(t)}.$$
(6)

Finally, for hosts using an avoidance resistance strategy,

$$\rho(t) = \rho(N, I, \bar{\beta}) = \bar{r}_{\beta}(t) - \delta N(t) - \mu - \alpha \frac{I(t)}{N(t)}. \quad (7)$$

Simulations elucidate how equations (5)-(7) affect recovery dynamics. Host populations using a tolerance strategy recovered (at the median) four times more slowly than host populations using an avoidance resistance strategy, all else being equal (fig. 3A). The faster recovery of hosts using an avoidance resistance strategy can be understood by equation (7). For a population evolving avoidance resistance, recovery (i.e., $\rho(t) > 0$) is driven by I/N decreasing because α remains fixed. The mechanism through which prevalence I/N decreases is negative selection on β : reducing β (increasing avoidance resistance) reduces pathogen R_0 , which reduces I/N. Eventually $R_0 < 1$ and I/N goes to zero, such that per capita growth rate $\rho(t)$ is no longer influenced by infection.

We can understand how prevalence I/N changes with changing β by examining a bifurcation plot of equation (3)

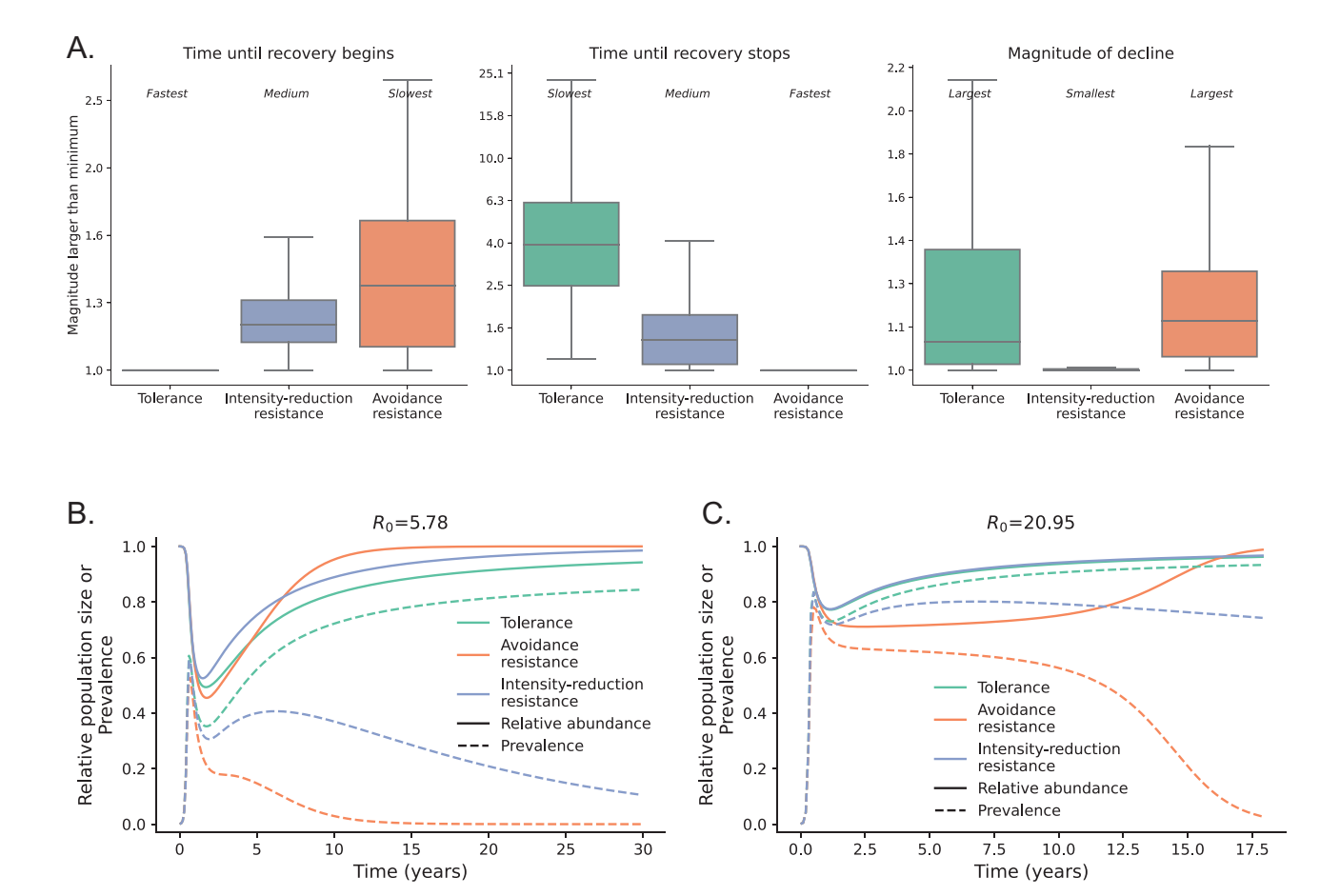


Figure 3: A, Comparison of time until recovery begins, time until recovery stops, and magnitude of decline between host populations using tolerance, avoidance resistance, and intensity-reduction resistance strategies, all else being equal. The boxplots are a result of 1,000 simulations with different parameter values. For each simulation, all three host defense strategies were compared to the minimum value for that simulation. The minimum strategy had a value of 1, and the other two strategies had values greater than 1. This was repeated 1,000 times. For example, a median value of ≊1.4 for the avoidance resistance strategy and the characteristic "time until recovery begins" indicates that avoidance resistance strategies have a median time until recovery begins that is 1.4 times slower (i.e., a larger value) than the defense strategy with the fastest time until recovery begins. Note that parameter combinations resulting in $R_0 > 20$ are excluded from the analysis. Boxes give the interquartile range, and whiskers are ±1.5 times the interquartile range. B, Example recovery trajectories from tolerant and resistant populations where the resistant populations recover more quickly than the tolerant population. Parameter values: $r = 4.69 \text{ yr}^{-1}$, $\mu = 2.73 \text{ yr}^{-1}, \, \delta = 0.25 \text{ area yr}^{-1}, \, \alpha = 2.30 \text{ yr}^{-1}, \, \omega = 451.55 \text{ yr}^{-1}, \, \mu_z = 29.89 \text{ yr}^{-1}, \, \beta = 0.25 \text{ area yr}^{-1}, \, \text{coefficient of variation in } \alpha, \, \beta,$ or $\hat{\alpha} = 0.54$. C, Same as B, but where a tolerant population recovers more quickly than or equivalently to the resistant populations. Parameter values: $r = 4.91 \text{ yr}^{-1}, \ \mu = 1.43 \text{ yr}^{-1}, \ \delta = 0.41 \text{ area yr}^{-1}, \ \alpha = 1.13 \text{ yr}^{-1}, \ \omega = 404.16 \text{ yr}^{-1}, \ \mu_z = 17.15 \text{ yr}^{-1}, \ \beta = 0.27 \text{ area yr}^{-1}, \text{ coefficients}$ ficient of variation in β or $\alpha = 0.62$. In B and C, solid lines show relative population size, and dashed lines show pathogen prevalence. These plots were made using equation (2) for tolerance, equation (3) for avoidance resistance, and equation (4) for intensity-reduction resistance.

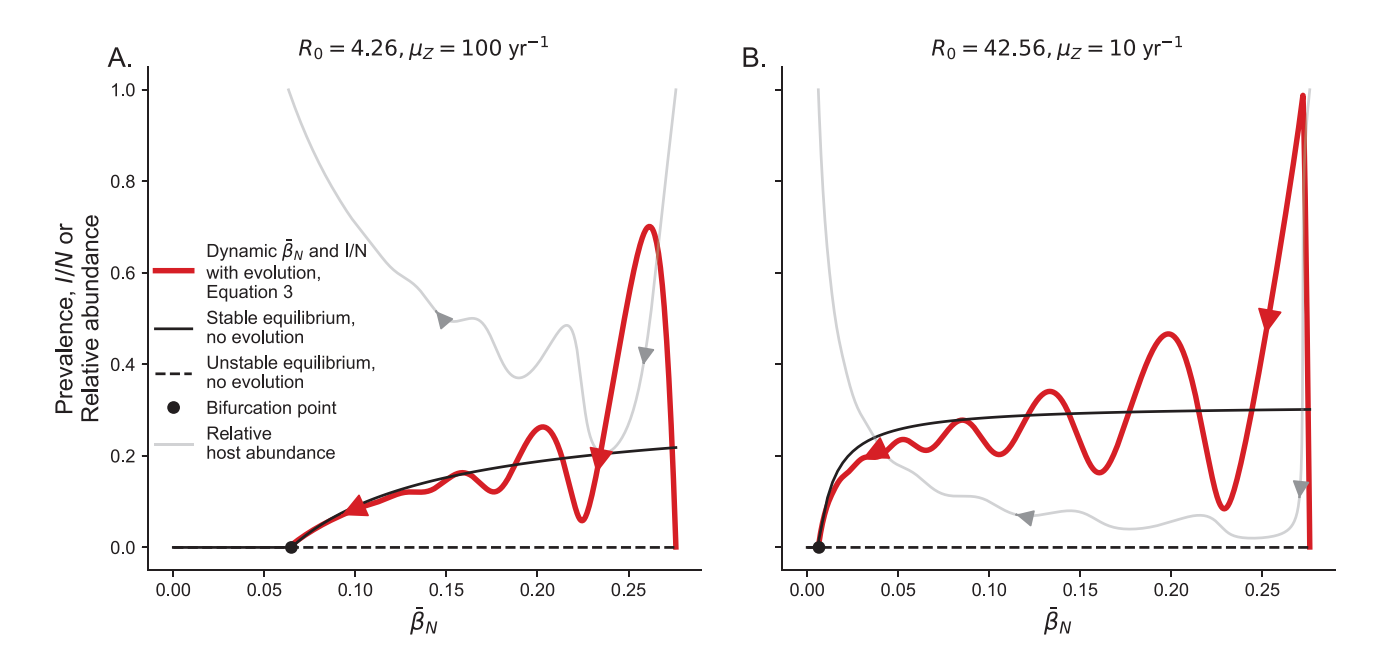


Figure 4: A, Example of how the evolution of avoidance resistance and the dynamics of host recovery can be understood in terms of a bifurcation plot. The black lines give the equilibria values of equation (3) when there is no variability and thus no evolution for a fixed $\bar{\beta}_N$ (solid lines are stable equilibria, and dashed lines are unstable equilibria). Varying $\bar{\beta}_N$ changes the equilibrium pathogen prevalence I^*/N^* in a population. A transcritical bifurcation point exists at $R_0=1$, below which the pathogen-free equilibrium is stable. The red line shows the dynamics of $\bar{\beta}_N$ and prevalence I(t)/N(t) when there is evolution in resistance. Time moves in the directions given by the red arrow (i.e., a population starts with $\bar{\beta}_N=0.276$, and $\bar{\beta}_N$ decreases through time due to evolution with subsequent changes in prevalence I(t)/N(t)). Host abundance relative to the predecline level is shown by the gray line. B, Same as A, but the death rate of the pathogen in the environment has been reduced by a factor of 10, with subsequent changes in the shape of the bifurcation diagram that have notable affects on the dynamics of host recovery trajectories. The values of other parameters are $r=1.68 \text{ yr}^{-1}$, $\mu=0.56 \text{ yr}^{-1}$, $\delta=0.14 \text{ area yr}^{-1}$, $\alpha=3.59 \text{ yr}^{-1}$, $\lambda=800 \text{ yr}^{-1}$, initial $\bar{\beta}=0.276 \text{ area yr}^{-1}$, and coefficient of variation in $\beta=0.32$.

without evolution, where β is the bifurcation parameter and the equilibrium of interest is equilibrium prevalence I^*/N^* (fig. 4A). Plotting the dynamics of β_N and I/N with evolution on the bifurcation plot, we see that the dynamics of evolving β_N and prevalence tend to track the bifurcation plot—in other words, we can conceptualize the dynamics of evolving β_N and I/N as similar to how a perturbation of fixed β affects equilibrium pathogen prevalence I^*/N^* . Using this insight, figure 4A shows that host recovery begins to happen before $R_0 < 1$ and evolution of β_N tends to stop once R_0 < 1 (with some overshoot depending on the speed of the evolutionary dynamics compared with the epidemiological dynamics). Moreover, as β_N gets closer to the bifurcation point, a change in β leads to a greater change in I/N (i.e., a steeper slope), leading to faster host recovery (fig. 4A).

In contrast, recovery for a tolerant population is driven strictly by a reduction in α because I/N will generally increase over time (eq. [5]; fig. 3A; reducing α increases pathogen R_0 , increasing prevalence I/N). While higher prevalence I/N increases the selection gradient on α and speeds up evolution (eq. [2]), the selection gradient is also

decreased by a reduction in the variance of α and slows down evolution (eq. [2]). The selection gradient on $\bar{\alpha}_N$ becomes increasingly weak as the variance in α also decreases. Thus, infection generally continues to dampen the per capita growth rate $\rho(t)$ of tolerant hosts for a longer time than resistant hosts, leading to slower recovery of tolerant hosts.

Recovery rates for host populations using an intensity-reduction resistance strategy are intermediate between tolerance and avoidance resistance strategies (a median of 1.38 times slower than the fastest recovery strategy; fig. 3A, 3B). When prevalence is more sensitive to changes in transmission, the recovery trajectories of intensity-reduction resistance can resemble avoidance resistance, leading to faster recovery rates (fig. 3B). However, when reductions in pathogen shedding (as a result of the evolution of intensity-reduction resistance) have little effect on pathogen prevalence (e.g., because of long pathogen persistence in the environment), the recovery of populations using intensity-reduction strategies can still occur because of reductions in disease-induced mortality rates (eq. [6]). Thus, intensity-reduction resistance recovery

rates mirror tolerance recovery rates in situations where prevalence is insensitive to changes in transmission (fig. 3C).

In contrast, the recovery rate of host populations using an avoidance resistance strategy can be drastically reduced when prevalence is insensitive to changes in transmission. For example, when pathogen death rate in the environment μ_z is low and R_0 is high, the bifurcation plot in figure 4B shows that prevalence is largely insensitive to small changes in β . This means that $\bar{\beta}_N$ has to be reduced to very low levels before there is a sufficient change in prevalence to allow intrinsic growth rate $\rho(t)$ to be greater than zero and host recovery to occur. In this situation, populations evolving avoidance resistance recover more slowly than populations evolving tolerance or intensityreduction resistance (fig. 3C).

Finally, hosts employing tolerance or avoidance resistance strategies did not differ consistently in the magnitude of decline experienced but did experience consistently larger declines than host populations using intensity-reduction resistance strategies (median declines were 1.1 times larger; fig. 3A). Across the parameter space we explored, hosts using tolerance strategies generally began recovering sooner following declines than hosts using avoidance or intensityreduction resistance strategies (fig. 3A).

Question 3: Trade-Offs between Host Defense and Fecundity Affect Recovery Dynamics but Have Little Effect on Disease-Induced Declines

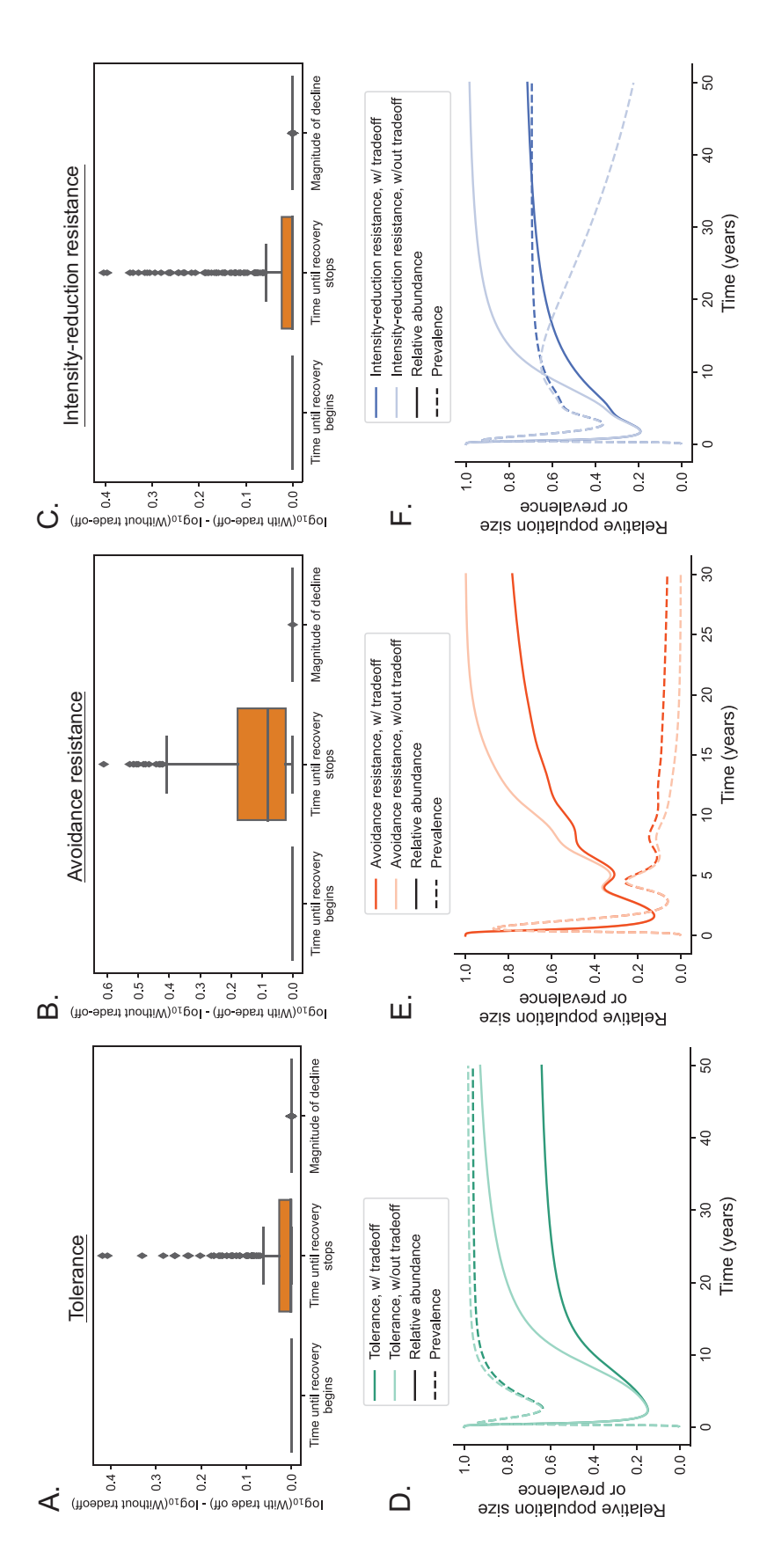
The time until recovery begins and the magnitude of decline were largely unaffected by the trade-off between host defense and fecundity (fig. 5A-5C). In contrast, our model predicted that time until recovery to some fixed point (which we set as within 2% of the equilibrium population size of the model with a host defense-fecundity trade-off and was less than the equilibrium abundance in the model without a trade-off) was slower in the populations with a trade-off (fig. 5A-5C). Host populations with a trade-off had a slower maximum per capita growth rate $\rho(t)$ after recovery (fig. 5D-5F). For tolerant host populations, the slower recovery rate was because α could not continue to decrease to zero given the trade-off $r(\alpha)$ (fig. 5D). As shown via Price's equation (supplemental PDF, sec. S3, eq. [S34]), the negative selection gradient on α is canceled out by the positive selection gradient induced by the trade-off $r(\alpha)$. For host populations using avoidance resistance, the slower recovery was also due to β not being able to be reduced enough such that $R_0 < 1$, allowing for persistence of the pathogen and host and a continued effect of infection on per capita host growth rate $\rho(t)$ (fig. 5*E*). Intensityreduction resistance was a combination of both of these mechanisms. The parameter $\hat{\alpha}$ could not go to zero because

of the trade-off (supplemental PDF, sec. S2, eq. [S42]) and prevalence also maintained a nonzero value (fig. 5F), both of which reduced $\rho(t)$.

Discussion

Motivated by disease-induced declines and ongoing recoveries in amphibian-fungal pathogen systems that are putatively driven by the evolution of host defense, we used a simple model to test how host life history, pathogen life history, standing genetic variation, host defense strategies, and trade-offs affected the dynamics of population recovery. Predictably, host life history defined along a slow-to-fast continuum was a strong predictor of host recovery trajectories. After accounting for differences in recovery due to host life history and standing genetic variation, we found that the type of host defense strategy strongly influenced multiple characteristics of a population's recovery trajectory. In single-species populations, resistance strategies tended to lead to faster recoveries than tolerance strategies. Thus, even when populations are deterministically predicted to recover to their predecline state, different strategies of host defense can lead to populations taking drastically different routes. This is important because spending a longer time below a critical population threshold can, for example, significantly augment the risk of stochastic extirpation and limit a population's ability to respond to secondary stressors (Lande et al. 2003). Last, we found that while trade-offs between host defense and fecundity slowed recovery rates for all defense strategies, they had little affect on short-term characteristics of population recovery trajectories.

Our results align with previous work on the long-term equilibrium outcomes of resistance and tolerance evolution (Antonovics and Thrall 1994; Roy and Kirchner 2000; Miller et al. 2005; Boots et al. 2009). For example, our model predicted that when there are no trade-offs, polymorphism in avoidance resistance was maintained because selection pressure induced by the pathogen effectively ended once mean avoidance resistance in the population was such that pathogen $R_0 < 1$ (fig. S2; Antonovics and Thrall 1994). Moreover, when a trade-off was present between fecundity and avoidance resistance such that pathogen persistence was possible, our model showed that resistance traits tended to fixation (fig. S3). While previous models have shown that trade-offs can promote equilibrium polymorphism in resistance traits within a population (Roy and Kirchner 2000), this primarily occurs when one of the possible host states is complete resistance with no intermediate options (e.g., $\beta = 0$). In contrast, when incomplete resistance states exist in the population, fixation of resistance is possible (fig. S3; Roy and Kirchner 2000).



termine when recovery stopped was the equilibrium host abundance of the population with a trade-off following pathogen invasion and recovery (specifically, when host abundance was within 2% of this value). B, Same as A, but for host populations using an avoidance resistance strategy. C, Same as B, but for host populations using an intensity-reduction resistance strategy. D, Example recovery trajectories of host populations using a tolerance strategy with and without a trade-off between fecundity and tolerance. Parameters used are $\alpha_m = 0.359$ E. Example recovery trajectories of host populations using an avoidance resistance strategy with and without a trade-off between fecundity and resistance. Parameters used are the same Figure 5: A, Comparison of 500 recovery trajectories of hosts using a tolerance strategy with and without a trade-off between tolerance and fecundity. When comparing two recovery trajectories with and without a trade-off, all parameters were identical other than the presence of the trade-off given by equation (S26) in section S2 of the supplemental PDF. The time yr^{-1} , $\omega = 843 \ yr^{-1}$, $\mu = 50 \ yr^{-1}$, $\tau = 1.68 \ yr^{-1}$, $\mu = 0.56 \ yr^{-1}$, initial coefficient of variation in $\alpha = 0.5$, initial mean $\alpha = 3.59 \ yr^{-1}$, $\delta = 0.14$ area yr^{-1} , and $\beta = 0.276$ area yr^{-1} . until recovery begins, the time until recovery to a fixed value, and the magnitude of decline were compared between the two recovery trajectories. The fixed value that was used to deas above but with $\beta_m=0.0276$. F, Example recovery trajectories of host populations using an intensity-reduction resistance strategy with and without a trade-off between fecundity and resistance. Parameters used are the same as above but with $\hat{\alpha}_m = 0.359$.

The primary goal of our study was to move beyond equilibrium results and elucidate the differences in the transient dynamics of host population recovery under tolerance and resistance strategies. We found that host populations employing different resistance strategies (avoidance and intensity-reduction resistance) often recovered drastically faster than populations using a tolerance strategy. The reason for this relates to the distinct mechanisms through which tolerant and resistant hosts evolve. For tolerant hosts, recovery trajectories are not driven by evolutionaryinduced reductions in pathogen fitness. Rather, pathogen fitness increases such that until a host evolves perfect tolerance, the pathogen will continue to negatively affect host fitness. Moreover, a key result of this work is that through our moment closure approximation we highlight a dampening feedback in tolerance evolution that affects the potential speed of population recovery. As mean tolerance in the population increases, variance in tolerance in the population decreases, slowing the speed at which mean tolerance can further increase. Together, this dampens the rate at which host populations evolving tolerance strategies can recover, compared with recovery in resistance populations and disease-free populations.

In contrast, the recovery trajectories of host populations using avoidance and intensity-reduction resistance are driven by a reduction in pathogen fitness, resulting in decreased pathogen prevalence and increased per capita host growth rate. However, a surprising result of this study was that for avoidance resistance in particular, ecological conditions greatly affected the sensitivity of prevalence to a change in avoidance resistance. For example, when pathogens could persist for long periods of time in the environment, a small evolutionary change in avoidance resistance had a negligible effect on pathogen prevalence and thus did relatively little to augment population recovery. In this situation, a host population's mean avoidance resistance value had to evolve close to a bifurcation point before any substantial host recovery could occur. This resulted in a type of slow-fast transient dynamics (Hastings et al. 2018), where host populations using avoidance resistance strategies could remain at seemingly stable low densities for long periods before rapidly recovering to predecline abundances. Interestingly, while we did not consider the evolution of the pathogen in this model, the prolonged persistence of pathogens in the environment can in some situations lead to an increase in pathogen virulence (Gandon 1998). The evolution of increased pathogen virulence could increase the selection gradient on host avoidance resistance, which could reduce the time that hosts evolving avoidance resistance spend in abundance troughs. Analyzing the transient dynamics of host recovery trajectories given the coevolution of hosts and pathogens is an interesting future direction (e.g., using a framework like that in Gandon and Day 2009).

Our results for avoidance resistance have important implications in multispecies systems. The ability of a host species using an avoidance resistance strategy to recover following disease-induced declines could be severely hindered by the presence of a species using a tolerance strategy even if these two species are demographically and ecologically equivalent. This is a transient manifestation of apparent competition (Holt and Pickering 1985), as ultimately both species have the evolutionary ability to deterministically recover to their predecline abundance but the recovery trajectory of the species using an avoidance resistant strategy can be drastically altered by the tolerant

Recovery trajectories of host populations using intensityreduction resistance exhibit similar benefits to avoidance resistance (e.g., the potential for faster recovery than tolerance strategies) but are less affected by ecological context. This raises the following question: Is there an optimal recovery strategy, all else being equal? While more rigorous analysis is needed, our analyses suggest that intensityreduction resistance may often be the preferred strategy for three reasons. First, populations evolving intensityreduction resistance can recover at least as fast as tolerant populations and at best significantly more quickly. Second, the recovery rates of populations evolving intensityreduction resistance are less sensitive to ecological context than populations using avoidance resistance strategies, reducing the likelihood of being trapped in prolonged periods of low abundance. Finally, although the effect was small in our simulations, populations employing intensityreduction resistance consistently experience smaller diseaseinduced declines than equivalent populations using tolerance and avoidance resistance. While existing standing variation and evolutionary constraints will affect the optimal defense strategy in natural populations, populations evolving intensityreduction strategies can be more resilient in terms of resisting and recovering from disease-induced declines across varying ecological contexts.

Implications for Recoveries in Amphibian-Bd Systems

Our study was motivated by amphibian-Bd systems, where we have observed drastic declines and the nascent recoveries of amphibian populations and communities. While lacking some key realism of amphibian-Bd systems, our model still provides retrospective and prospective insight into amphibian recoveries. For mountain yellow-legged frog (MYL frog) populations in the Sierra Nevada mountains of California (composed of two sister species, Rana muscosa and Rana sierrae), there is strong evidence of population recoveries following Bd-induced declines (Knapp et al. 2016). Moreover, there is evidence that the evolution of intensity-reduction resistance and tolerance are, at least in part, driving these recoveries (Knapp et al. 2023). MYL frogs have a long-lived tadpole stage that does not suffer disease-induced mortality from infection and can prolong the persistence of Bd in this system (Briggs et al. 2010). It is therefore broadly consistent with our model results that we observe recovering populations in this system evolving intensity-reduction resistance and tolerance rather than avoidance resistance, as avoidance resistance could substantially delay recoveries and keep populations at low densities for long periods of time before recovery.

In Panamanian amphibian communities, where we are observing the recovery and reorganization of entire amphibian communities following Bd-induced declines (Voyles et al. 2018), the mechanisms of recovery remain unclear. However, our model makes at least two predictions that could inform our understanding of recovery mechanisms in this system. First, we predict that we are more likely to observe avoidance resistance as a mechanism of recovery in terrestrial host species that have less habitat overlap with viable, aquatic zoospores shed by other hosts in the community. As such, we would predict patterns of decreasing prevalence with increasing host abundance to be skewed toward more terrestrial species that interact less with the aquatic zoospore pool. Second, after controlling for host life history, we predict that primarily aquatic amphibian hosts with the highest recovery rates are more likely to be using tolerance or intensity-reduction resistance strategies. Thus, we predict that aquatic species with high recovery rates should generally maintain high Bd prevalence and show detectable reductions in infection intensity. It is important to note, however, that ecological interactions not accounted for in our current model could significantly alter these predictions. For example, interspecific competition among species could interact with standing variation in host defense to lead to transient recovery dynamics in host communities that differ significantly from equivalent single-species recovery trajectories. It will be important to extend the model we develop here to incorporate interacting species with varying host defense strategies to thoroughly explore the recovery and reorganization dynamics of communities in the presence of a pathogen.

Conclusions

A key goal in amphibian-Bd systems, as well as in host-pathogen systems more generally, is to identify the mechanisms leading to recovery (Brannelly et al. 2021). The theory developed here highlights that there are distinct signatures of different host defense strategies embedded in the transient trajectories of prevalence, infection intensity, and host abundance during host recovery. A key contribution of this study is that we show that the recovery tra-

jectories of host abundance can differ drastically across defense strategies and that these differences can be highly influenced by environmental conditions. Importantly, given that we can control for host life history (e.g., by leveraging a priori information on host vital rates and demographic structure), we can use the results of this theory in combination with observed patterns of prevalence, infection intensity, and, in particular, host abundance to statistically compare among candidate defense strategies driving host recoveries. This provides an exciting opportunity to empirically test the extent to which different species and even populations of the same species use different defense strategies to resist and recover from disease-induced declines.

Acknowledgments

Funding for this work was provided by National Science Foundation grant DBI-2120084. Thanks to members of the Resilience Institute Bridging Biological Training and Research (RIBBiTR) for useful discussions and feedback. Thanks to reviewers whose comments improved the study.

Statement of Authorship

All authors contributed to conceptual development. M.Q.W. and S.S. performed the analyses. M.Q.W. and J.A.D. wrote the first draft. All authors contributed to revisions.

Data and Code Availability

No data were used in this article. All code necessary to reproduce the results in this article is available on Zenodo (https://zenodo.org/doi/10.5281/zenodo.10475490; Wilber et al. 2024).

Literature Cited

Agrawal, A., and C. M. Lively. 2002. Infection genetics: gene-for-gene versus matching-alleles models and all points in between. Evolutionary Ecology Research 4:79–90.

Alizon, S., A. Hurford, N. Mideo, and M. Van Baalen. 2009. Virulence evolution and the trade-off hypothesis: history, current state of affairs and the future. Journal of Evolutionary Biology 22:245–259.

Anderson, R. M., and R. M. May. 1982. Coevolution of hosts and parasites. Parasitology 85:411–426.

Antonovics, J., and P. H. Thrall. 1994. The cost of resistance and the maintenance of genetic polymorphism in host-pathogen systems. Proceedings of the Royal Society B 257:105–110.

Ballard, P. G., N. G. Bean, and J. V. Ross. 2016. The probability of epidemic fade-out is non-monotonic in transmission rate for the Markovian SIR model with demography. Journal of Theoretical Biology 393:170–178.

- Berngruber, T. W., R. Froissart, M. Choisy, and S. Gandon. 2013. Evolution of virulence in emerging epidemics. PLoS Pathogens 9:e1003209.
- Blehert, D. S., A. C. Hicks, M. Behr, C. U. Meteyer, B. M. Berlowski-Zier, E. L. Buckles, J. T. H. Coleman, et al. 2008. Bat white-nose syndrome: an emerging fungal pathogen? Science 323:227.
- Bolker, B., and S. W. Pacala. 1997. Using moment equations to understand stochastically driven spatial pattern formation in ecological systems. Theoretical Population Biology 52:179-197.
- Bonnet, T., M. B. Morrissey, P. de Villemereuil, S. C. Alberts, P. Arcese, L. D. Bailey, S. Boutin, et al. 2022. Genetic variance in fitness indicates rapid contemporary adaptive evolution in wild animals. Science 376:1012-1016.
- Boots, M., A. Best, M. R. Miller, and A. White. 2009. The role of ecological feedbacks in the evolution of host defence: what does theory tell us? Philosophical Transactions of the Royal Society B
- Boots, M., and R. G. Bowers. 1999. Three mechanisms of host resistance to microparasites—avoidance, recovery and tolerance show different evolutionary dynamics. Journal of Theoretical Biology 201:13-23.
- Boots, M., and Y. Haraguchi. 1999. The evolution of costly resistance in host-parasite systems. American Naturalist 153:359-
- Brannelly, L. A., H. I. Mccallum, L. F. Grogan, C. J. Briggs, M. P. Ribas, M. Hollanders, T. Sasso, M. Familiar Lopez, D. A. Newell, and A. M. Kilpatrick. 2021. Mechanisms underlying host persistence following amphibian disease emergence determine appropriate management strategies. Ecology Letters 24:130-148.
- Briggs, C. J., R. A. Knapp, and V. T. Vredenburg. 2010. Enzootic and epizootic dynamics of the chytrid fungal pathogen of amphibians. Proceedings of the National Academy of Sciences of the USA 107:9695-9700.
- Bruns, E., M. E. Hood, and J. Antonovics. 2015. Rate of resistance evolution and polymorphism in long- and short-lived hosts. Evolution 69:551-560.
- Byrne, A. Q., C. L. Richards-Zawacki, J. Voyles, K. Bi, R. Ibáñez, and E. B. Rosenblum. 2021. Whole exome sequencing identifies the potential for genetic rescue in iconic and critically endangered Panamanian harlequin frogs. Global Change Biology 27:50-70.
- Capdevila, P., I. Stott, M. Beger, and R. Salguero-Gómez. 2020. Towards a comparative framework of demographic resilience. Trends in Ecology and Evolution 35:776-786.
- Cortez, M. H., and M. A. Duffy. 2021. The context-dependent effects of host competence, competition, and pathogen transmission mode on disease prevalence. American Naturalist 198:179-
- Cunningham, C. X., S. Comte, H. McCallum, D. G. Hamilton, R. Hamede, A. Storfer, T. Hollings, et al. 2021. Quantifying 25 years of disease-caused declines in Tasmanian devil populations: host density drives spatial pathogen spread. Ecology Letters 24:958-
- Day, T., and S. Gandon. 2007. Applying population-genetic models in theoretical evolutionary epidemiology. Ecology Letters 10:876-
- DiRenzo, G. V., E. F. Zipkin, E. H. Grant, J. A. Royle, A. V. Longo, K. R. Zamudio, and K. R. Lips. 2018. Eco-evolutionary rescue promotes host-pathogen coexistence. Ecological Applications 28:1948-1962.

- Duffy, M. A., and S. E. Forde. 2009. Ecological feedbacks and the evolution of resistance. Journal of Animal Ecology 78:1106-
- Epstein, B., M. Jones, R. Hamede, S. Hendricks, H. McCallum, E. P. Murchison, B. Schonfeld, C. Wiench, P. Hohenlohe, and A. Storfer. 2016. Rapid evolutionary response to a transmissible cancer in Tasmanian devils. Nature Communications 7:12684.
- Gandon, S. 1998. The curse of the pharaoh hypothesis. Proceedings of the Royal Society B 265:1545-1552.
- Gandon, S., P. Agnew, and Y. Michalakis. 2002. Coevolution between parasite virulence and host life-history traits. American Naturalist 160:374-388.
- Gandon, S., and T. Day. 2009. Evolutionary epidemiology and the dynamics of adaptation. Evolution 63:826-838.
- Gignoux-Wolfsohn, S. A., M. L. Pinsky, K. Kerwin, C. Herzog, M. Hall, A. B. Bennett, N. H. Fefferman, and B. Maslo. 2021. Genomic signatures of selection in bats surviving white-nose syndrome. Molecular Ecology 30:5643-5657.
- Golas, B. D., B. Goodell, and C. T. Webb. 2021. Host adaptation to novel pathogen introduction: predicting conditions that promote evolutionary rescue. Ecology Letters 24:2238-2255.
- Hastings, A., K. C. Abbott, K. Cuddington, T. Francis, G. Gellner, Y. C. Lai, A. Morozov, S. Petrovskii, K. Scranton, and M. L. Zeeman. 2018. Transient phenomena in ecology. Science 361: eaat6412.
- Hodgson, D., J. L. McDonald, and D. J. Hosken. 2015. What do you mean, "resilient"? Trends in Ecology and Evolution 30:503-506.
- Holland, O. J., M. Toomey, C. Ahrens, A. A. Hoffmann, L. J. Croft, C. D. Sherman, and A. D. Miller. 2022. Whole genome resequencing reveals signatures of rapid selection in a virus-affected commercial fishery. Molecular Ecology 31:3658-3671.
- Holt, R. D., and J. Pickering. 1985. Infectious disease and species coexistence: a model of Lotka-Volterra form. American Naturalist 126:196-211.
- Hoyt, J. R., A. M. Kilpatrick, and K. E. Langwig. 2021. Ecology and impacts of white-nose syndrome on bats. Nature Reviews Microbiology 19:196-210.
- Ingrisch, J., and M. Bahn. 2018. Towards a comparable quantification of resilience. Trends in Ecology and Evolution 33:251-259.
- Joseph, M. B., and R. A. Knapp. 2018. Disease and climate effects on individuals drive post-reintroduction population dynamics of an endangered amphibian. Ecosphere 9:e02499.
- Kerr, P. J. 2012. Myxomatosis in Australia and Europe: a model for emerging infectious diseases. Antiviral Research 93:387-415.
- Kilpatrick, A. M., C. J. Briggs, and P. Daszak. 2010. The ecology and impact of chytridiomycosis: an emerging disease of amphibians. Trends in Ecology and Evolution 25:109-118.
- Knapp, R. A., G. M. Fellers, P. M. Kleeman, D. A. Miller, V. T. Vredenburg, E. B. Rosenblum, and C. J. Briggs. 2016. Largescale recovery of an endangered amphibian despite ongoing exposure to multiple stressors. Proceedings of the National Academy of Sciences of the USA 113:11889-11894.
- Knapp, R. A., M. B. Joseph, T. C. Smith, E. E. Hegeman, V. T. Vredenburg, J. E. Erdman Jr., D. M. Boiano, A. J. Jani, and C. J. Briggs. 2022. Effectiveness of antifungal treatments during chytridiomycosis epizootics in populations of an endangered frog. PeerJ
- Knapp, R. A., M. Q. Wilber, A. Q. Byrne, M. B. Joseph, T. C. Smith, A. P. Rothstein, R. L. Grasso, and E. B. Rosenblum. 2023. Evolutionary rescue and reintroduction of resistant frogs

- allows recovery in the presence of a lethal fungal disease. bioRxiv, https://doi.org/10.1101/2023.05.22.541534.
- Lande, R., S. Engen, and B.-E. Sæther. 2003. Stochastic population dynamics in ecology and conservation. Oxford University Press, Oxford
- Langwig, K. E., W. F. Frick, J. R. Hoyt, K. L. Parise, K. P. Drees, T. H. Kunz, J. T. Foster, and A. M. Kilpatrick. 2016. Drivers of variation in species impacts for a multi-host fungal disease of bats. Philosophical Transactions of the Royal Society B 371:20150456.
- Lion, S., and J. A. Metz. 2018. Beyond R_0 maximisation: on pathogen evolution and environmental dimensions. Trends in Ecology and Evolution 33:458–473.
- Marino, S., I. B. Hogue, C. J. Ray, and D. E. Kirschner. 2009. A methodology for performing global uncertainty and sensitivity analysis in systems biology. Journal of Theoretical Biology 254:178– 196.
- McMahon, T. A., B. F. Sears, M. D. Venesky, S. M. Bessler, J. M. Brown, K. Deutsch, N. T. Halstead, et al. 2014. Amphibians acquire resistance to live and dead fungus overcoming fungal immunosuppression. Nature 511:224–227.
- Medzhitov, R., D. S. Schneider, and M. P. Soares. 2012. Disease tolerance as a defense strategy. Science 335:936–941.
- Mendelson, J. R., S. M. Whitfield, and M. J. Sredl. 2019. A recovery engine strategy for amphibian conservation in the context of disease. Biological Conservation 236:188–191.
- Miller, M. R., A. White, and M. Boots. 2005. The evolution of host resistance: tolerance and control as distinct strategies. Journal of Theoretical Biology 236:198–207.
- ———. 2006. The evolution of parasites in response to tolerance in their hosts: the good, the bad, and apparent commensalism. Evolution 60:945–956.
- 2007. Host life span and the evolution of resistance characteristics. Evolution 61:2–14.
- Neubert, M. G., and H. Caswell. 1997. Alternatives to resilience for measuring the responses of ecological systems to perturbations. Ecology 78:653–665.
- Orr, H. A., and R. L. Unckless. 2014. The population genetics of evolutionary rescue. PLoS Genetics 10:e1004551.
- Osnas, E. E., P. J. Hurtado, and E. E. Osnas. 2015. Evolution of pathogen virulence across space during an epidemic. American Naturalist 185:332–342.
- Raberg, L., A. L. Graham, and A. F. Read. 2009. Decomposing health: tolerance and resistance to parasites in animals. Philosophical Transactions of the Royal Society B 364:37–49.
- Roy, B. A., and J. W. Kirchner. 2000. Evolutionary dynamics of pathogen resistance and tolerance. Evolution 54:51–63.

- Scheele, B. C., F. Pasmans, L. F. Skerratt, L. Berger, A. Martel, W. Beukema, A. A. Acevedo, et al. 2019. Amphibian fungal panzootic causes catastrophic and ongoing loss of biodiversity. Science 363:1459–1463.
- Searle, C. L., and M. R. Christie. 2021. Evolutionary rescue in host-pathogen systems. Evolution 75:2948–2958.
- Tobler, U., A. Borgula, and B. R. Schmidt. 2012. Populations of a susceptible amphibian species can grow despite the presence of a pathogenic chytrid fungus. PLoS ONE 7:e34667.
- Valenzuela-Sánchez, A., M. Q. Wilber, S. Canessa, L. D. Bacigalupe, E. Muths, B. R. Schmidt, A. A. Cunningham, A. Ozgul, P. T. Johnson, and H. Cayuela. 2021. Why disease ecology needs lifehistory theory: a host perspective. Ecology Letters 24:876–890.
- Voyles, J., D. C. Woodhams, V. Saenz, A. Q. Byrne, R. Perez, G. Rios-Sotelo, M. J. Ryan, et al. 2018. Shifts in disease dynamics in a tropical amphibian assemblage are not due to pathogen attenuation. Science 359:1517–1519.
- Vredenburg, V. T., R. A. Knapp, T. S. Tunstall, and C. J. Briggs. 2010. Dynamics of an emerging disease drive large-scale amphibian population extinctions. Proceedings of the National Academy of Sciences of the USA 107:9689–9694.
- White, J. W., C. Barceló, A. Hastings, and L. W. Botsford. 2022. Pulse disturbances in age-structured populations: life history predicts initial impact and recovery time. Journal of Animal Ecology 91:2370–2383.
- Wilber, M. Q., J. A. DeMarchi, C. J. Briggs, and S. Streipert. 2024. Data from: Rapid evolution of resistance and tolerance leads to variable host recoveries following disease-induced declines. American Naturalist, Zenodo, https://zenodo.org/doi/10.5281/zenodo.10475490.
- Wilber, M. Q., P. T. J. Johnson, and C. J. Briggs. 2019. When chytrid fungus invades: integrating theory and data to understand disease-induced amphibian declines. Pages 511–543 in K. Wilson, A. Fenton, and D. M. Tompkins, eds. Wildlife disease ecology: linking theory to data and application. Cambridge University Press, Cambridge.

References Cited Only in the Online Enhancements

Meyer, K. 2016. A mathematical review of resilience in ecology. Natural Resource Modeling 29:339–352.

Associate Editor: Luděk Berec Editor: Erol Akçay